

Hybrid SALP Swarm Grey Wolf Optimized Fuzzy Based Maximum Power Point Tracking in Photovoltaic Panel

Mintu Kumar^{1*}, Ritula Thakur²

¹M.E. Scholar*, Department of Electrical Engineering, National Institute of Technical Teachers Training and Research (NITTTR), Chandigarh, India, mintu.elect20@nitttrchd.ac.in

²Associate Professor, Department of Electrical Engineering, National Institute of Technical Teachers Training and Research (NITTTR), Chandigarh, India, ritula@nitttrchd.ac.in

ARTICLE INFO

ABSTRACT

Received: 19 Dec 2024

Revised: 18 Feb 2025

Accepted: 28 Feb 2025

The global need for renewable energy sources (RES) is increasing day by day, as the degradation of fossil fuel is happening in the environment. There were many RES available such as wind, solar, hydropower, geothermal, and biomass among them the solar energy was regarded as the sustainable to satisfy the energy demand. Because of its cheap maintenance, long lifespan, and cleanliness, solar photovoltaic (PV) systems are becoming more and more popular among RES. The primary goal of the proposed system is to expand array efficiency by optimizing the performance of fuzzy-based maximum power point tracking (MPPT) controllers using a hybrid approach that combines Salp Swarm Optimization (SSO) and Grey Wolf Optimization (GWO). The proposed hybrid optimization algorithm effectively tunes the parameters of the fuzzy logic controller (FLC), this leads to improve the tracking performance. This leads to a robust and efficient MPPT controller using fuzzy logic to accurately track the MPP under unpredictable ecological circumstances. The proposed method values are given to the Simulink/Matlab environment, and the results are taken. The efficiency obtained by the proposed system is 99.8% and the power obtained is 3995W. The proposed method efficiently tracks the performance of the MPPT.

Keyword: Renewable Energy Source, Solar Photovoltaic, FLC, MPPT, Boost Converter, Salp Swarm, and Grey Wolf Optimization.

1. Introduction

The population of the earth continues to grow, and the demand for energy rises accordingly [1]. However, conventional energy sources such as uranium, oil, coal, and natural gas are limited in supply [2]. This emphasizes the need to adopt alternative energy solutions. Renewable energy sources (RES) are becoming increasingly important in generating electricity to meet this demand [3, 4]. Wind, solar PV, biomass, and fuel cells are renewable energy sources that can be utilized as alternatives for electricity generation, helping to fulfill our daily energy needs [5]. Solar energy is a great choice for electricity generation because it is clean, pollution-free, and widely accessible [6, 7]. Solar power is commonly used in industrial, commercial, residential, and military sectors. The performance of solar or photovoltaic (PV) cells in generating electricity is affected by environmental factors like sunlight intensity, angle, cell temperature, and load conditions [8].

The main benefit of PV power generation systems is their ability to produce high-output power, ranging from kilowatts to megawatts. This makes PV energy suitable for various applications, such as communications, space vehicles, water pumping, reverse osmosis plants, satellite systems, and power plants [9]. A solar PV array transforms sunlight into electrical energy [10, 11]. While its efficiency is lower compared to other renewable energy sources, it can perform more effectively if it continuously adjusts to eco-friendly modifications, such as disparities in solar radiation and temperature, to optimize power output [12]. The efficacy of a PV system can be amended by implementing an MPPT. The MPPT is a technique used for maximizing the output power of the array to adjust the voltage and current relationship, thereby boosting the system's overall power [13].

An MPPT controller is necessary for a solar-based PV system to operate at peak efficiency and increase production. This demonstrates that, despite varying weather, the PV module consistently runs at its maximum power output [14]. Because it can be difficult to keep track of the maximum power point, various strategies have been developed to enhance system efficiency. These strategies include techniques like Fractional Open-Circuit Voltage (FOCV), Fractional Short-Circuit Current (FSCC), Fuzzy Logic, Neural Networks, Perturbation

and Observation (P&O), and Incremental Conductance algorithms [15]. Author [16] utilized the fuzzy-based solar MPPT for the application of electric vehicle (EV). In [17], the simulation of solar PV with MPPT by utilizing fuzzy logic control (FLC) approach. Author [18] described the performance analysis of artificial neural networks (ANN) and P&O based on MPPT in PV systems. In [19], particle swarm optimization (PSO) was employed to maximize the power in solar PV applications. The author [20] utilized the MPPT for tracing the Global maximum power point (GMPP) by using PSO. The above-mentioned strategies have several limitations, like high costs, complexity, trouble in implementation and possible unpredictability. To address these limitations, this research proposes the optimization of a fuzzy-based MPPT controller for solar PV schemes by utilizing SSO and GWO to maximize power generation. The main objectives of our proposed system are,

- To increase the efficacy of solar based PV systems by optimizing the performance of fuzzy-based MPPT controllers through a hybrid optimization technique (SGWO).
- To advance a robust and efficient MPPT controller using fuzzy logic to accurately track the MPP under varying eco-friendly settings.
- To propose a hybrid optimization algorithm (SGWO) to effectively adjust the parameters of the FLC, leading to improved tracking performance.
- To solve the performance of the proposed optimized controller in terms of power extraction efficiency, and speed tracking, against ecological variations.

The organization of this paper is described as follows: section 2 explains the various related works based on MPPT. The proposed approach is detailed in Section 3, which covers the modeling of the PV system, battery, and fuzzy-based MPPT controllers through a hybrid optimization of salp swarm and grey wolf optimization. The simulation outcomes are described in section 4. Finally, a conclusion with future research is providing in section 5.

2. Literature Survey

Some of the existing works related to the MPPT with different controlling strategies are discussed in this section. Hussaian Basha et al. [21] discussed tracking the PV power using hybrid MPPT based on partial shading conditions. The Hybrid optimization techniques for MPPT were evaluated by examining various aspects such as the presence of oscillations at the MPP, the effectiveness of power extraction, the time required to reach the MPP, and their reliance on the PV model. The hybrid MPPT method that combines Modified Grey Wolf Optimization (MGWO) with ANFIS demonstrates higher performance than other power point tracking methods.

Mariprasath et al. [22] explained in PV to maximize the output power using cuckoo search optimization (CSO). The MPPT was utilized for Solar PV topology to optimize the power output, ensuring peak performance under both constant and varying climatic conditions. A stackable single-switch boost converter (SSBC) with a Cuckoo Search MPPT controller was suggested for the Solar PV system. The efficacy of this design was compared with the traditional boost converters utilizing different MPPT techniques.

For MPPT in the PVA, Manna et al. [23] developed a model reference adaptive control (MRAC) design. To improve MPPT performance, simplify system control, and efficiently handle environmental uncertainties and disturbances in the PV system, a new adaptive control framework was put into place. The results demonstrated that the suggested controller provides excellent tracking performance across different conditions, including in the change of irradiance and temperature. The proposed MPPT topology achieves the lowest oscillation at the MPP, faster convergence, improved efficiency, minimal ripple, and a lower error rate when compared to others. Viswa Teja et al. [24] explained the ANN-based MPPT in the solar-battery powered EVs Permanent Magnet Synchronous (PMS) motor. An ANN-based MPPT controller is applied to enhance the operation of the solar PV array and maximize the output. A solar battery powered battery EV with ANN based MPPT control system was designed. The performance of the suggested system was assessed by examining data gathered under various load conditions to ensure stable parameters like torque and speed.

Mallat et al. [25] discussed the MPPT for the extraction of maximum power in PV system with genetic algorithm (GA) based. The boost converter was adjusted with the duty cycle with GA-based MPPT algorithm, allowing PV modules to activate at their MPP. The PV conversion platform was designed using Simulink/Matlab software. The result showed that the viability of the suggested method has higher efficiency in regulating an off-grid PV system.

Areola et al. [26] explained the MPPT based Adaptive Neuro-fuzzy inference system (ANFIS) in the solar PV scheme. The irradiance and temperature data were obtained through the online global database. The ANFIS reference model was developed using solar irradiance and temperature as input parameters, with the reference maximum power output as the output parameter. The results verified that the suggested topology was more

efficient than other traditional methods. Table 1 represents the methods, advantages, and disadvantages of different references.

Table 1. Methods of different references.

References	Method	Advantages	Disadvantages
Hussaian Basha et al. [21]	MGWO -ANFIS	Higher performance	High computational complexity
Mariprasath et al. [22]	CSO based MPPT	To optimize the power output, ensuring peak performance	Overfitting issues
Manna et al. [23]	MRAC	To optimize MPPT performance, simplifying system control	Limited to designing an MRAC-based MPPT specifically for partial shading conditions
Viswa Teja et al. [24]	ANN based MPPT	Improved the operation of the solar PV array and maximize its output	Computational overhead
Mallat et al. [25]	GA-based MPPT	High efficiency	High computational complexity
Areola et al. [26]	ANFIS	Highly efficient	Overfitting issues

3. Proposed Methodology

Global attempts to investigate RES counting wind, solar, biomass, hydropower, and geothermal have increased due to the environment's degradation from global warming, the rising need for energy, and the depletion of fossil fuel supplies. In particular, solar energy is regarded as a sustainable power-generating alternative because of its global availability and environmental advantages. Because of its cheap maintenance, long lifespan, and cleanliness, solar photovoltaic (PV) systems are becoming more popular among RESs. However, variable climatic factors like partial shadowing, which can produce several points on the power-voltage (P-V) curve, pose efficiency issues for PV systems. The MPPT methods are employed to optimize energy extraction from PV arrays. The development of metaheuristic procedures, such as genetic algorithms (GA) and PSO, which provide better tracking performance but have certain limitations, resulted from the inability of conventional MPPT algorithms to accurately determine the true maximum power point in partial shading situations. Thus, this research work proposed the optimization of **fuzzy-based MPPT controllers** for solar PV systems using **hybrid salp swarm optimization and grey wolf optimization (HSSGWO)** for maximum power generation. The PV module's output is linked to a DC-DC converter, which receives voltage and power change signals from the input block and relays them to a fuzzy logic controller (FLC). The FLC output is then supplied to the output block, which modulates the signal with an appropriate repetitive sequencing signal. To enhance flexibility and efficiency, an optimized approach is introduced for configuring FLC system parameters using a cascaded optimization algorithm. This hybrid algorithm fine-tunes the FLC parameters, ensuring precise and rapid tracking of the desired outcomes. Fig. 1 below illustrates the block diagram of the suggested topology.

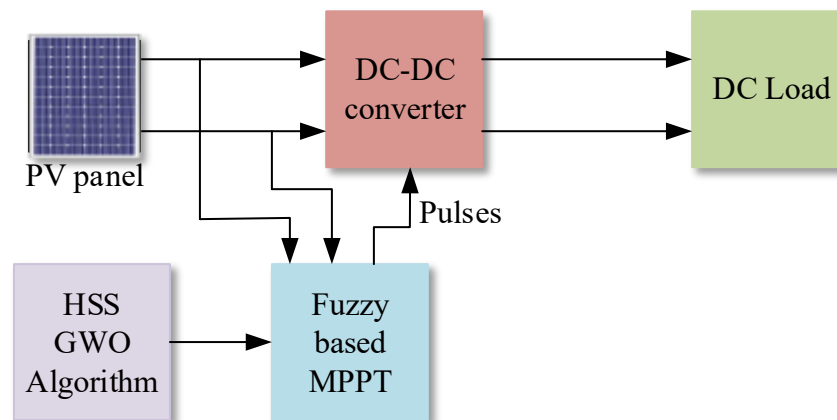


Fig. 1. Block diagram for the proposed system

3.1 PV Modeling

The source of energy from the sun is fed to the solar panel. The solar panel receives the irradiance from the sun, and the atoms in the panel are energized and tend to move [27]. This leads to the formation of an energy source in the panel. The below-given Fig. 2 represents the modeling circuit of the PV panel [28].

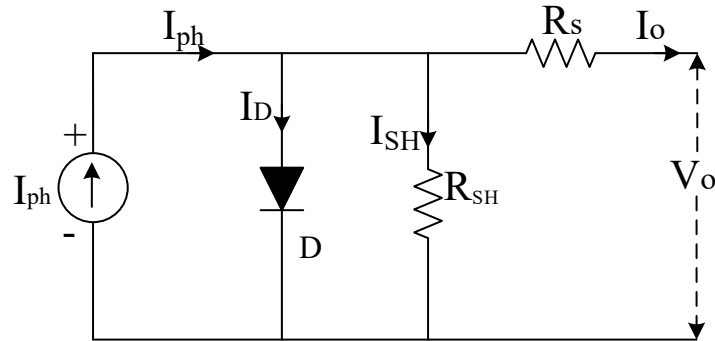


Fig. 2. Circuit model of PV panel.

The above figure (2) has a diode current represented as I_D , shunt current is represented as I_{SH} and series resistance is represented as R_s . In the above figure, by applying the Kirchhoff's law at the node is derived in the equation below equation (1),

$$I_{ph} = I_D + I_{SH} + I_o \quad (1)$$

From the equation (1), the equation (2) is given by,

$$I_o = I_{ph} - I_D - I_{SH} \quad (2)$$

The photovoltaic current source equation (2) is given, the supply requires maintaining a balance of the equation between the cell and the parallel resistance.

$$I_o = I_{ph} - I_0 \left[\exp \left(\frac{V_o + I_o * R_s}{V_T} \right) - 1 \right] - \left[\frac{V_o + I_o * R_s}{R_{SH}} \right] \quad (3)$$

The above equation (3) illustrates the current value for the PV system. I_0 exemplifies the reverse saturation current, and V_o represents the voltage produced in the system. After the generation of power in the panel, a system is required to extract the power [29]. The boost converter is a device for boosting out the potential from the PV. For the ideal model of the PV panel, a diode is placed in parallel with the system. The power generated in the panel is not balancing so there is a series and shunt resistance is used in the system.

3.2 Boost Converter

A DC-DC step-up converter is utilized in the system to extract the MPP from the PV; it is positioned between the PV and the load. It is employed to maximize solar panel load matching. To increase the power generated in the PV panel, the converter duty cycle D is used in the selection process, and the IGBT is used to enhance the converter parameters and control [30]. The equation below describes the output for voltage and current of the boost converter are given by equation (4 and 5),

$$V_o = V_i \frac{1}{1-d} \quad (4)$$

$$I_o = I_i (1-d) \quad (5)$$

Here, in the boost converter the V_o and I_o are given as the outputs, V_i and I_i are given as the inputs for both voltage and current and d is the duty cycle of the boost converter.

3.3 MPPT

To take the power output from the system to the fullest is described in this technique. The MPPT is mainly used in PV, wind turbines, optical power transmission, and thermo photovoltaic. The working principle of the MPPT is that it detects the output current and voltage of the irradiance method to calculate their power and decide whether the system is in MPP. The MPPT regulates the voltage and current separately, which aids in managing the suggested system's overall performance [31]. This can be achieved by, controlling the MPPT with the help of an algorithm. In the MPPT, the algorithm used in the proposed paper is FLC.

3.4 FLC

Three major components make up FLC. The fuzzy transforms the crisp variables into fuzzy or linguistic variables in the first section. The IF-THEN rule based on the FLC is combined with fuzzy inference in the second portion of the fuzzy. In the third part defuzzification is used to convert the linguistic variables back into crisp variables.

3.4.1 Proposed MPPT control based on HSSGWO and FLC

When faced with unexpected changes in the weather, FLCs are more intelligent and resilient than other controllers like MPPT controllers. In this proposed system, the MPPT controller is optimized with FLC and hybrid SSO and GWO (HSSGWO). The controller is an offline-based controller, and the computational cost is not analyzed. Since the controller determines the duty cycle for the DC-DC converter by applying fuzzy rules, its design phase should be based on fuzzy logic principles. In order to construct a Fuzzy system, it is necessary to define the inputs and outputs, as well as their membership functions and definition scope.

Fuzzy inputs are defined in this proposed study as the ratio of power variations to voltage variations and the derivative of this ratio, both of which are considered to be fuzzy. Since D is the desired value for the controller design, it follows that the output of the fuzzy system should likewise be set to D. Therefore, the fuzzy system has two inputs and an output. The fuzzy system uses triangle membership functions for both its input and output. The triangle membership function uses the symmetrical phase system to specify the ranges of the variables. The range variables are ranged from 3 membership function as an input and 9 membership function for output.

The MPPT operates based on the PV module of the PV characteristic. In FLC, the input to the controller is given by, E and dE in equation (6) and (7). The rate of power to voltage variations and the difference of E at time t_r , correspondingly [32]. The output obtained by the controller is a duty cycle given in the equation (6 and 7).

$$E(t_r) = \frac{G_{po}(t_r) - G_{po}(t_r - 1)}{V_{po}(t_r) - V_{po}(t_r - 1)} \quad (6)$$

$$dE(t_r) = E(t_r) - E(t_r - 1) \quad (7)$$

Here, $G_{po}(t)$ and $V_{po}(t)$ are the output power voltage of the PV module are given in the system.

3.4.2 Definition of Membership Function

In this process, the first stage is to identify the description series and the membership function in input and output of FLC. The variables obtained in the system are 5 and given as the input to the membership function and the 17 defined variables are obtained and given as the output to the membership function and they are all identical through an optimization process. The below Fig. 3 describes the membership function for 5 variables ($x(1)$ to $x(5)$) the signs are given as negative (N), zero (Z), and positive (P). The place of these parameters should be optimized for the finest outcome.

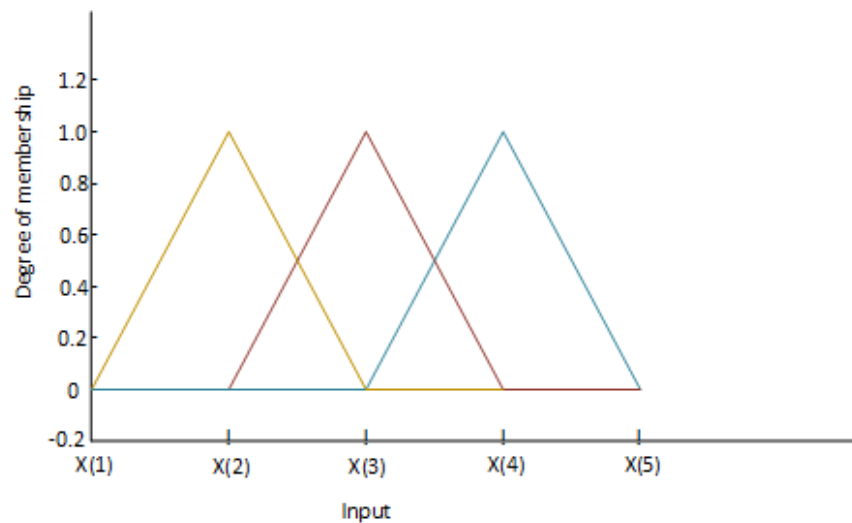


Fig. 3. Sample of FLC membership function

3.4.3 Design of Fuzzy Rule Set

The fuzzy rule set is given in the second phase and is the greatest significant phase of FLC and in the design of the FLC. Mamdani defuzzification is utilized in this work. In this system the fuzzy input is divided into three membership function then the fuzzy rule is considered to be nine rules which is listed in table 2. Here, X(28) to X(36) as the optimization variables in the fuzzy set rules to determine their optimal values. The optimization variables of the membership function in this system take 10 inputs, 17 outputs, and 9 variables utilized to determine fuzzy rules into account [33]. Table 2 represents the summary of FLC rules.

Table 2. Summary of FLC rules

D			E
dE is P	dE is Z	dE is N	
X(30)	X(29)	X(28)	N
X(33)	X(32)	X(31)	Z
X(36)	X(35)	X(34)	P

3.4.4 Definition of objective function

Defuzzification stands as the final stage of the objective function. Optimizing the error level of the fuzzy inputs E and dE is the main goal of the topology. The criterion error cost function is given as integral square error (ISE) in equation (8).

$$D(\Delta E) = \int_0^{G_s} (\Delta E^2 + \Delta dE^2) dt \quad (8)$$

Here, G_s is represented as the simulation time; ΔE and ΔdE represent the relation of power mismatch to voltage mismatch, and the derivation is also optimized.

3.5 Salp Swarm Optimization

The remaining salps in the chain follow the leader's movements, adjusting their positions based on a mathematical model that mimics their natural behavior. The optimization performance is enhanced by this coordinated movement, which allows for effective exploration of the search space. Because it strikes a good compromise between the two, the SSA method is good at addressing complicated optimization issues. The equation (9) represents the search of food.

$$X_{l_o}^1 = \begin{cases} f_{l_o}^* + C_{l_o}(ub_{l_o} - lb_{l_o})C_{2_o} + lb_{l_o}, C_{3_o} \geq 0.5 \\ f_{l_o}^* - C_{l_o}(ub_{l_o} - lb_{l_o})C_{2_o} + lb_{l_o}, C_{3_o} < 0.5 \end{cases} \quad (9)$$

C_{20} and C_{30} represents the selection of random number $[0, 1]$, X_{lo}^1 represents i^{th} coordinate for the salp leader and f_{lo}^* represents the food source.

Decreased as shown in equation (10) is the exploration and exploration ability balancing coefficient C_{lo} for SSA.

$$C_{lo} = 2e^{-\left(\frac{4t}{n}\right)^2} \quad (10)$$

Here, t represents the iteration formed and n illustrates the supreme amount of repetitions existent. As the leader is updated the followers, follow the same path as the leader [34]. The updating equation is given below equation (11),

$$X_{lo}^K = \frac{1}{2}(X_{lo}^K + X_{lo}^{K-1}) \quad (11)$$

Here, X_{lo}^K illustrates the location of the K^{th} follower at the I^{th} measurement and $I \geq 2$.

3.6 Grey Wolf Optimization

This meta-heuristic approach is based on grey wolf simulation. The grey wolf optimization (GWO) has solved many optimization problems of non-bulging and gave the finest result by comparing other optimizations such as PSO, GSA, and DE. The GWO has mainly three wolf search engines to search the entire space. The three search engines are alpha (α), beta (β), and gamma (γ). Alpha is the first among the three and the dominant leader followed by beta and the lowest is the gamma in the ranking system. Omega (ω) wolves are also present and are not as important as the other three as shown below in Fig. 4.

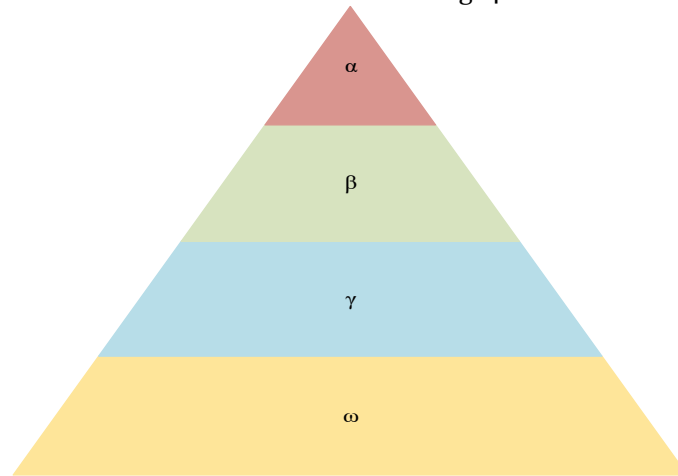


Fig. 4. Grey wolf hierarchy

The attacking pattern of the prey by the wolves is mainly divided into three stages. The insights of the hunting pattern are by finding the prey, encircling it, and disturbing it until they break off. The equation for encircling the prey is given below equation (12 and 13),

$$\vec{T} = \left| \vec{G} \cdot \vec{X}_p(t_r) - \vec{X}_{pV}(t_r) \right| \quad (12)$$

$$\vec{X}_{pV}(t_r + 1) = \vec{X}_p(t_r) - \vec{A} \cdot \vec{T} \quad (13)$$

In this equation \vec{T} represents the existing location, \vec{X}_p represents the location of target, \vec{X}_{pV} represents the location of the grey wolf, \vec{A} and \vec{G} are the constant courses and are intended as in equation (14 and 15),

$$\vec{A} = 2\vec{a} \cdot \vec{r}_1 - \vec{a} \quad (14)$$

$$\vec{G} = 2 \cdot \vec{r}_2 \quad (15)$$

Here, \vec{r}_1 and \vec{r}_2 represents the random value, and 'a' is varied from 2 to 0 at time of iteration [35]. As the engine don't know the exact position of the prey, they are going to employ the best hunter for the hunting behavior. The remaining position depends on the search engine. The hunting is normalized by hunting down the prey by best, subsequently best and the third best. The lowest wolf updates their equation (16, 17, and 18).

$$\begin{aligned}\vec{T}_\alpha &= \left| \vec{G}_1 \cdot \vec{X}_\alpha(t_r) - \vec{X}_{pV}(t_r) \right|, \\ \vec{T}_\beta &= \left| \vec{G}_2 \cdot \vec{X}_\beta(t_r) - \vec{X}_{pV}(t_r) \right|,\end{aligned}\quad (16)$$

$$\begin{aligned}\vec{T}_\gamma &= \left| \vec{G}_3 \cdot \vec{X}_\gamma(t_r) - \vec{X}_{pV}(t_r) \right| \\ \vec{X}_1 &= \vec{X}_\alpha - \vec{A}_1 \cdot (\vec{T}_\alpha), \\ \vec{X}_2 &= \vec{X}_\beta - \vec{A}_2 \cdot (\vec{T}_\beta),\end{aligned}\quad (17)$$

$$\begin{aligned}\vec{X}_3 &= \vec{X}_\gamma - \vec{A}_3 \cdot (\vec{T}_\gamma) \\ \vec{X}(t+1) &= (\vec{X}_1 + \vec{X}_2 + \vec{X}_3) / 3\end{aligned}\quad (18)$$

Here, $\vec{X} = 1, 2, 3, \dots, n$ represent the population, $\vec{X}_\alpha, \vec{X}_\beta, \vec{X}_\gamma$ are the search agents, respectively. The below-given Fig. 5 represents the flow chart for the suggested HSSGWO. This gives the detailed operation of the proposed topology.

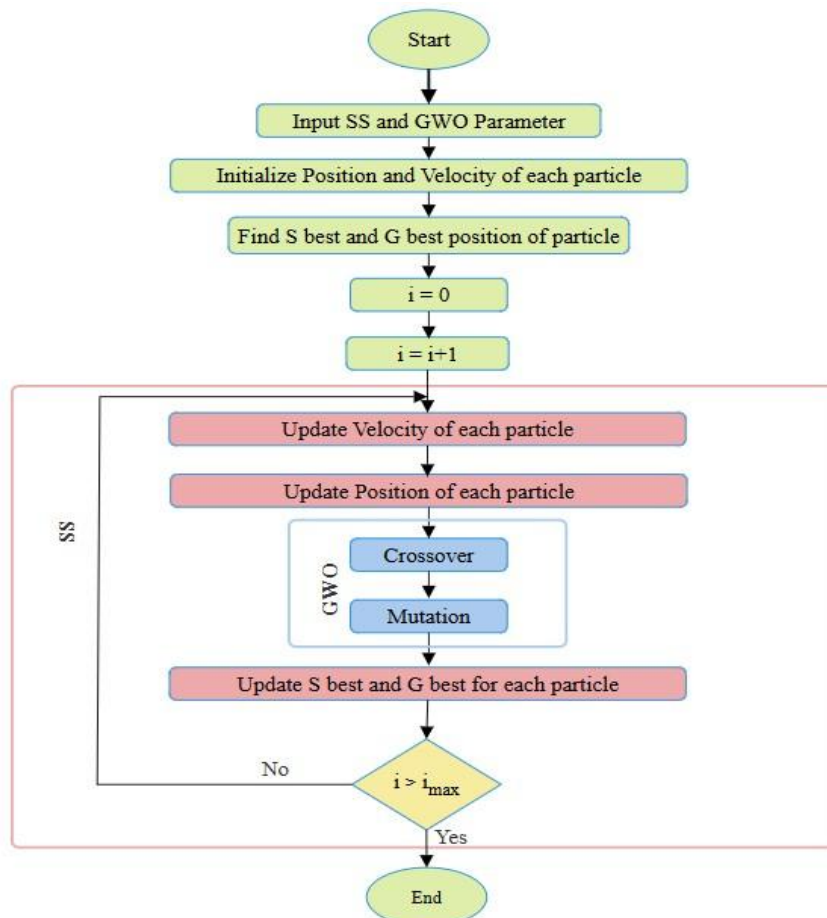


Fig. 5. Flow chart representation of HSSGWO

4. Results and discussions

The proposed system was simulated by the Simulink tool the required result was taken from the system. The input from the PV array is given to the DC-DC converter, the fuzzy-based MPPT sends the signal to the converter. The algorithm used in the proposed system is the hybrid salp swarm grey wolf optimization technique as shown below in Fig. 6. The signal is given to the fuzzy controller to tune the gain parameters.

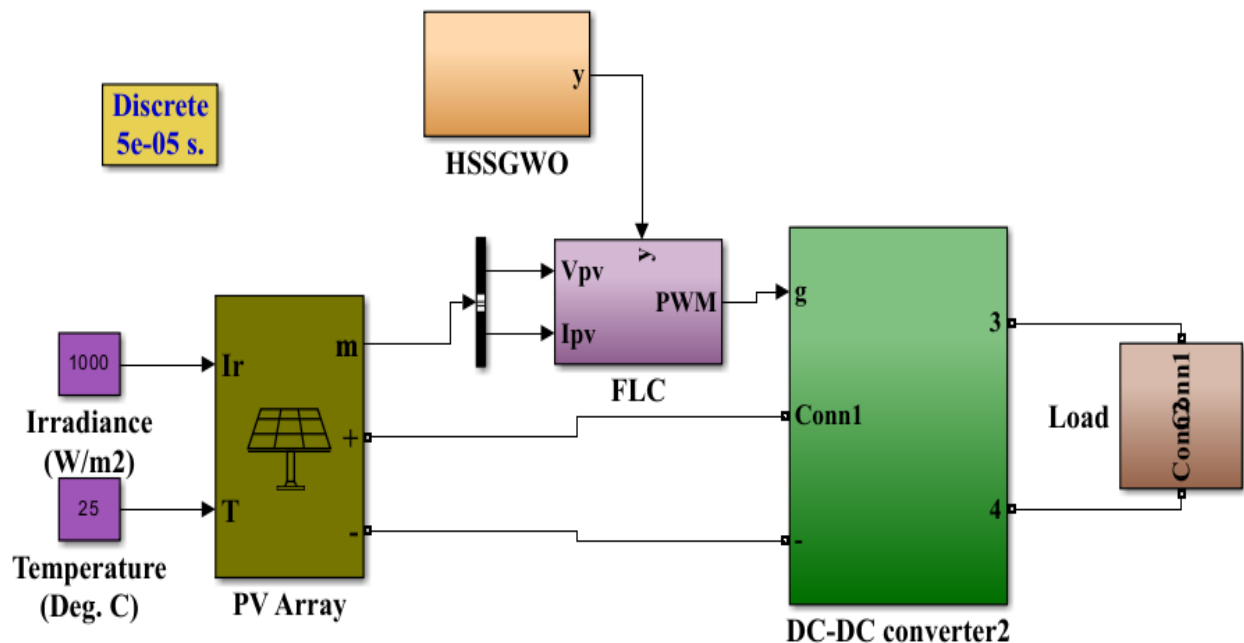


Fig. 6. Simulation of proposed topology

The input to the system is given as irradiance and temperature to the user-defined 5-module and 4 parallel panels. This is then fed to the DC-DC converter and to the load. The signal is also fed to the FLC and then given to the converter circuit. Then, they are given to the load. Below Table 3 represents the number of parameters and the value section that is described in the below section.

Table 3. Number of parameter and value

Value	Parameter
200.143 W	Maximum power
54 Ncell	Cells per module
32.9 Voc (V)	Open circuit voltage
8.21 Isc (A)	Short circuit voltage
26.3 V	Voltage at maximum power point
7.61 A	Current at maximum power point
-0.355 (%/deg.C)	Temperature coefficient of Voc
0.06 (%/deg.C)	Temperature coefficient of Isc

4.1 Case 1. Constant temperature irradiance

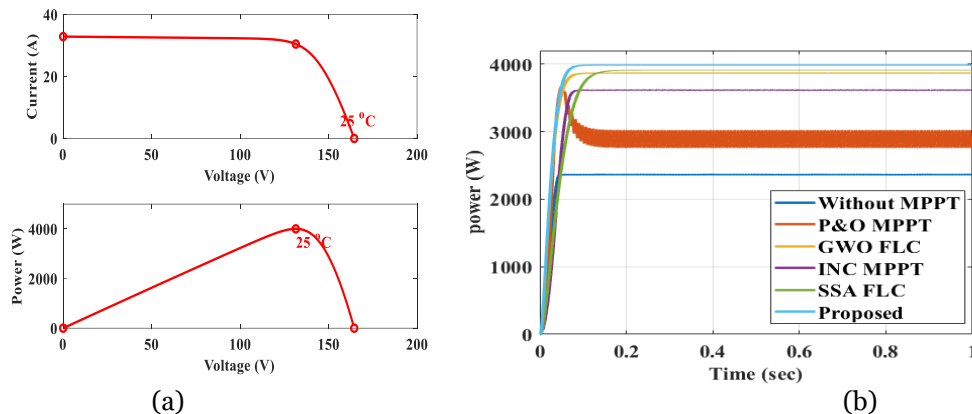


Fig. 7. Waveform for (a) Current and Power and (b) comparison for constant irradiance

The above Fig. 7 (a) represents the output waveform for power and current with constant irradiance 1000 W/m^2 and temperature 25°C . The current is flown through the constant system at 32.84A , the power is raised to 4000 W/m^2 and dropped at 164.5V . Therefore, the constant irradiance is formulated in the system. The above Fig. 7 (b) represents the comparison of power with different algorithms and controller and found that the proposed system has a continuous irradiance of 1000 W/m^2 , for the power of 4000W at a varying time. Below Table 4 represents the comparison of different algorithms for stable irradiance.

Table 4. Comparison of stable irradiance

Case1		
	Efficiency	Power
Proposed	99.8	3995
SSA	97.74	3912.5
GWO	96.8	3875
INC	90.335	3616
P&O	75.4	3020
Without MPPT	59.2	2370

4.2 Case 2. Varying irradiance

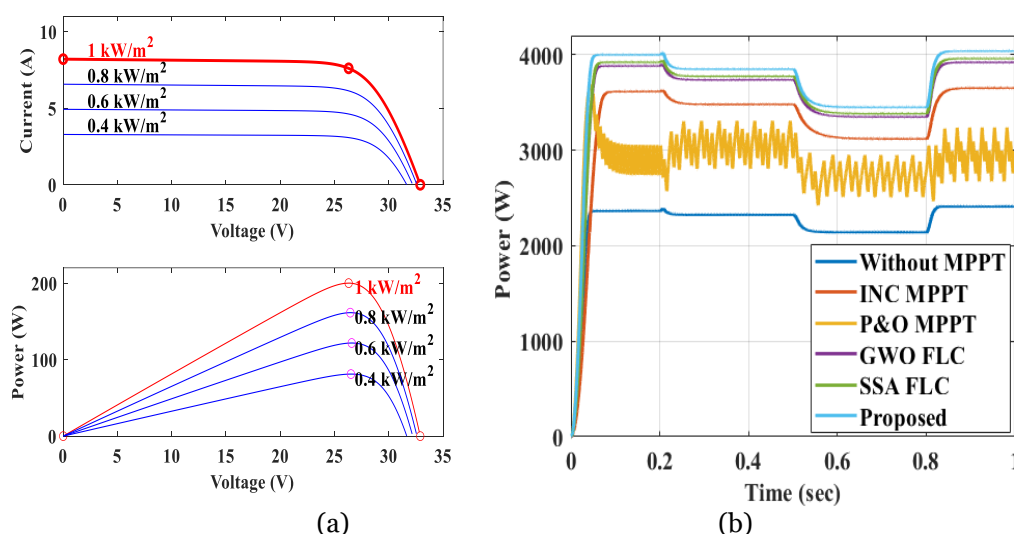


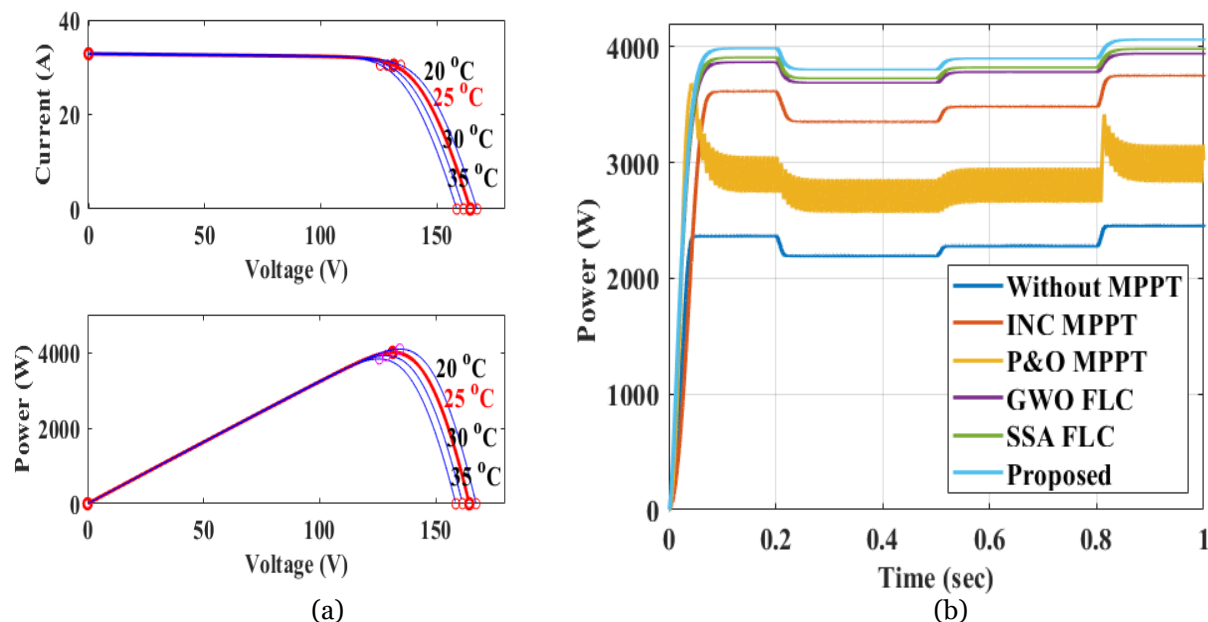
Fig. 8. Waveform for (a) Current and Power and (b) comparison for varying irradiance

The above Fig. 8 represents the output waveform of varying irradiance for (a) power and current, and (b) comparison for varying irradiance. In the proposed system the irradiance for 1000 W/m² with a current of 32.84A and a voltage of 164.5V is obtained in the system. For the comparison of varying irradiance, the time period of 0 to 0.2, 0.2 to 0.45, 0.45 to 0.8, and 0.8 to 1 gives the irradiance of 1000, 600, 400, and 800 W/m². Here, Table 5 represents the comparison variable irradiance of different times for different algorithms.

Table 5. Comparison of variable irradiance

Case2							
Time	Irradiance	Proposed	SSA	GWO	INC	P&O	Without
0-0.2	1000	99.82	97.76	96.93	90.29	75.3	59.2
0.2-0.5	600	93.89	91.41	93.1	87.9	81.16	55.2
0.5-0.7	400	91.09	89.3	87.43	82.4	72.13	53.6
0.8-1	800	95.23	93.23	94.2	88.493	79.2	58.41

4.3 Case 3. Varying temperature

**Fig. 9. Waveform for (a) Current and Power and (b) comparison for varying temperature**

The above Fig. 9 represents the output waveform of varying temperature for (a) power and current, and (b) comparison for varying temperature. For the current of 32.87A and power of 4002.86W, the temperature is varied such as 20, 25, 30, and 35°C in the above figure. In the comparison range the irradiance is varied with respect to the varying temperature. Here, the below Table 6 represents the comparison variable temperature of different time for the different algorithms.

Table 6. Comparison of variable temperature

Case 3							
time	Temperature	Proposed	SSA	GWO	INC	P&O	Without
0-0.2	35	98.5	98.07	98.9	94.36	78.3	61.6
0.2-0.5	30	97.03	95.11	94.21	85.56	68.93	55.91
0.2-0.8	25	97.6	95.43	94.43	86.9	69.9	56.83
0.8-1	20	99.5	97.35	96.37	91.7	73.3	59.92

4.4 Partial shading condition

In the partial shading state, here we use three panels for calculating the I-V characteristic and P-V features. The condition occurs when there is not much amount of irradiance formed by the sun though it is shaded by some kind of natural phenomenon. For bypassing this condition, the MPPT are used in the proposed system.

- Condition 2

- Condition 3
- Condition 1

4.4.1 Condition 1. Pattern with irradiance 1000 W/m^2 , 1000 W/m^2 , & 1000 W/m^2

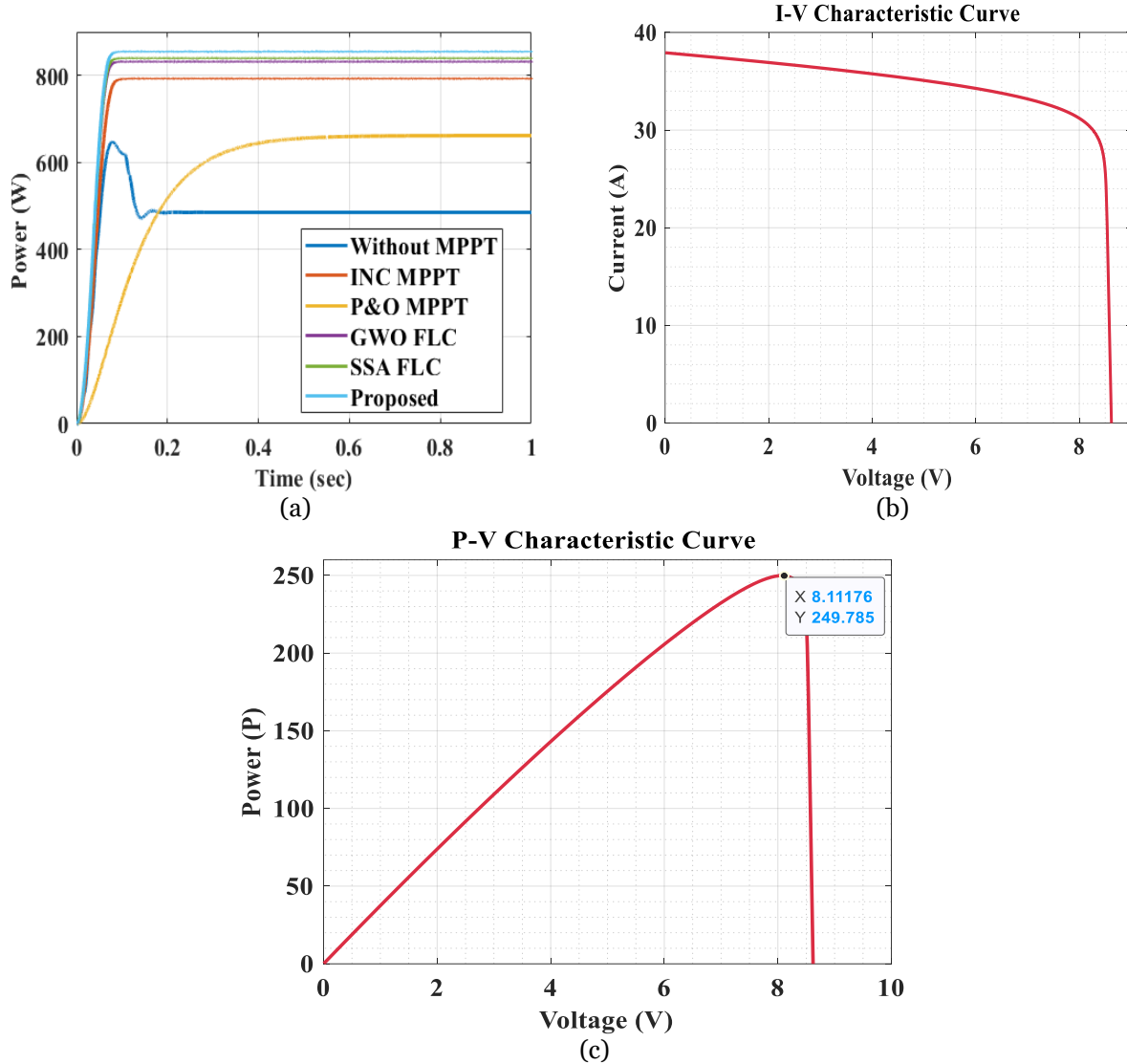


Fig. 10. Output waveform for partial shading condition 1 (a) comparison, (b) I-V, and (c) P-V
 In this condition, Fig. 10 represents the output waveform for the partial shading condition of I-V Characteristic, P-V Characteristic, and the comparison waveform. Here, three panels are used for the partial shading for a common and stable irradiance of 1000 W/m^2 . Each and every panel used the same irradiance of 1000 W/m^2 .

4.4.2 Condition 2. Pattern with irradiance 1000 W/m^2 , 1000 W/m^2 , & 400 W/m^2

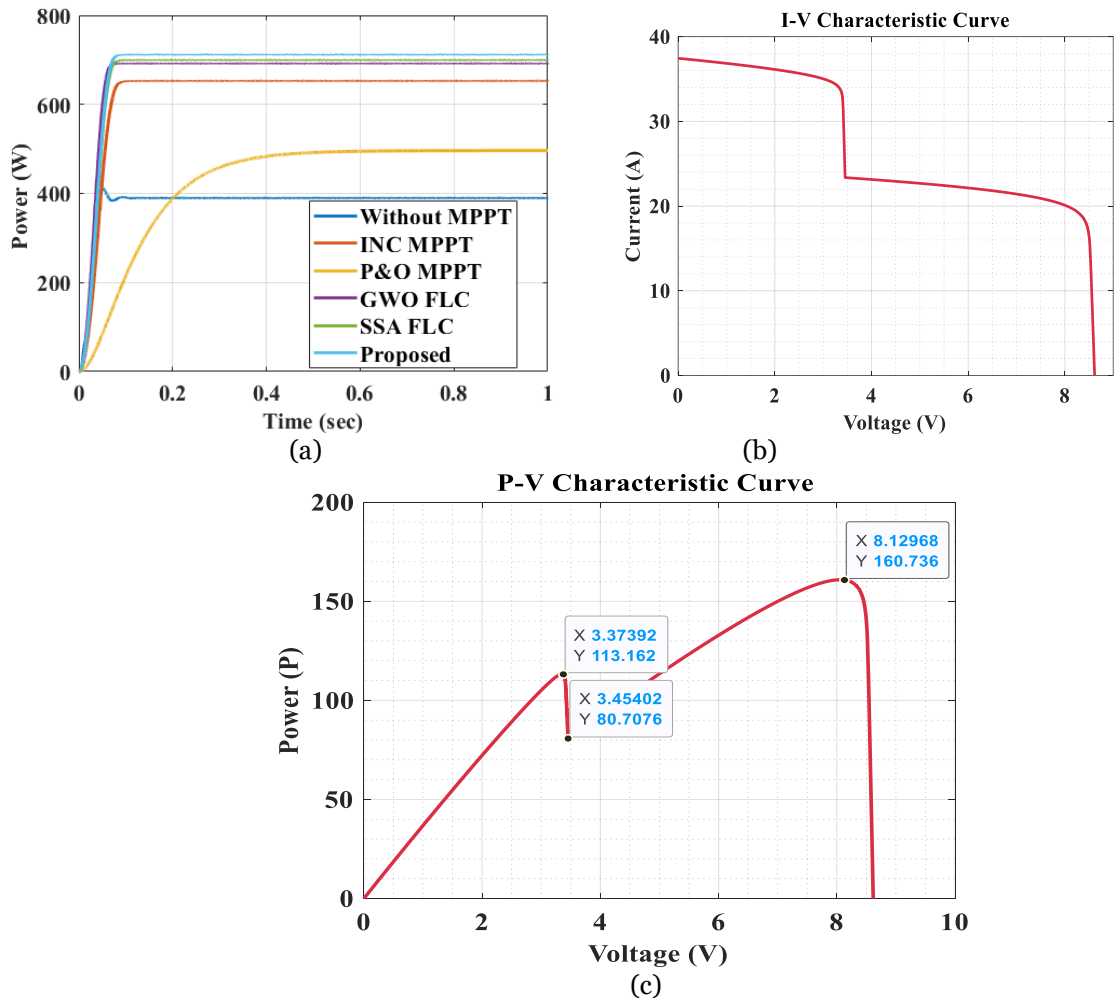
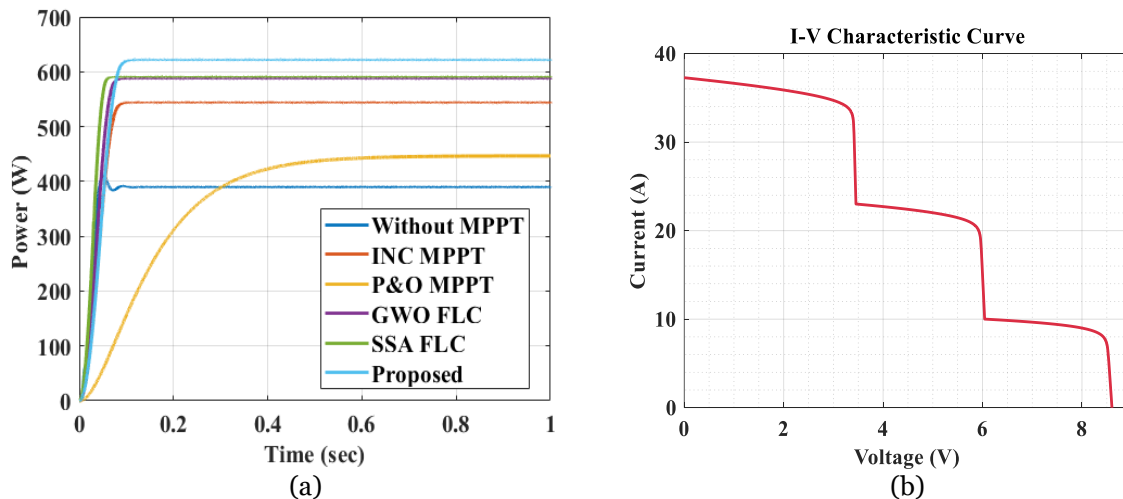


Fig. 11. Output waveform for partial shading condition 2 (a) comparison, (b) I-V, and (c) P-V

The above Fig. 11 represents the partial shading condition 2 for comparison, I-V characteristic and P-V characteristic curve. In this phase unlike condition 1 the third-panel irradiance is changed. The irradiance values applied in the three panels are 1000 W/m^2 , 1000 W/m^2 , and 400 W/m^2 .

4.4.3 Condition 3. Pattern with irradiance 1000 W/m^2 , 700 W/m^2 , & 400 W/m^2



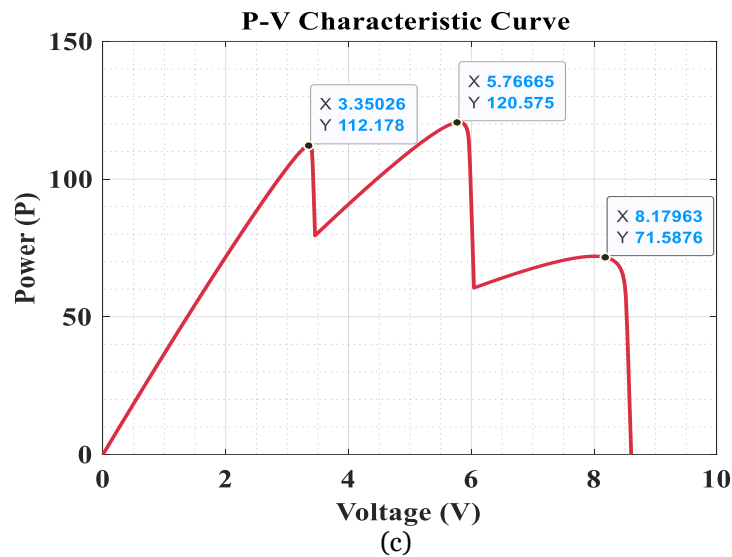


Fig. 12. Output waveform for partial shading condition 3 (a) comparison, (b) I-V, and (c) P-V

The above Fig. 12 represents the output waveform for partial shading condition 3 of I-V characteristic, P-V characteristic and the comparison is given. The irradiance for the three panels are different 1000 W/m^2 , 700 W/m^2 , and 400 W/m^2 .

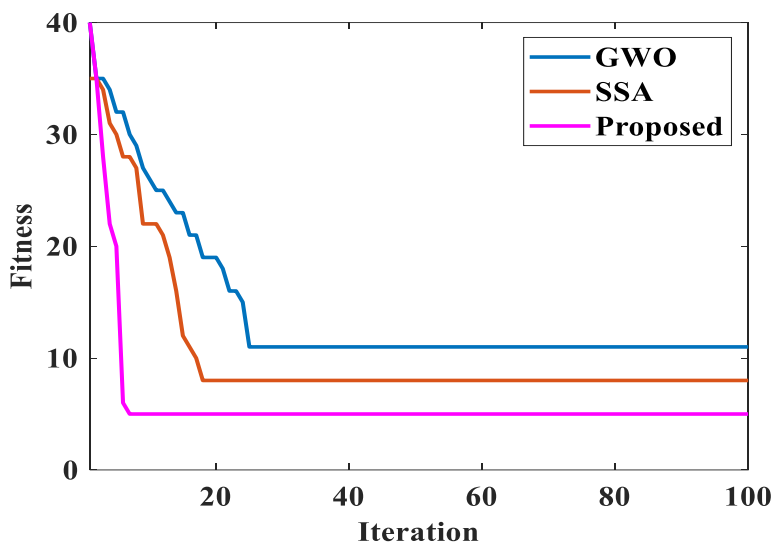


Fig. 13. Graphical representation for iteration

The proposed system is represented in the above-mentioned graphical Fig. 13 with the comparison of other mentioned grey wolf optimization and salp swarm optimization, and observed that our proposed system obtains less iteration. The below Table 7 illustrates the comparison of different algorithm with different time responses. From the comparison Table 7, it has been perceived that the suggested system has achieved in a smaller number of time while comparing with different topologies.

Table 7. Comparison of different algorithm with different time response

	Proposed	SSA	GWO	INC	P&O	Without
Rise time (Tr)	0.0383	0.0725	0.0416	0.0524	0.9885	0.9867
Peak time (Tp)	0.062	0.098	0.084	0.91	1.45	1.23
Settling time (Ts)	0.0578	0.068	0.0709	0.71	0.3	0.413
Peak overshoot (Mp)	2.44	0.32	-0.63	-0.728	-5.92	-39.2

5. Conclusion

The enhancement of PV by optimizing the performance of fuzzy-based MPPT controller through HSSGWO, to develop a robust and efficient use of MPPT controller to trace the maximum power point in different load conditions an FLC is used. Thus, the system can compare the performance of the suggested controller with the current techniques and assess how well the MPPT performs in terms of power extraction efficiency and speed tracking against environmental fluctuations. The efficiency obtained by the proposed system is 99.8% and the power obtained by the system is 3995W. The speed tracking of the system is observed and found the proposed system achieves improvement over the other system, and also in the comparison aspect the system performs better than the SSA, GWO, INC, P&O, and without MPPT. The future of this paper can be implemented in direct work. The optimization can be improved to give a 100% efficiency range.

Declaration of Competing Interest

The authors declare that they have no known competing financial interests or personal relationships that could have appeared to influence the work reported in this paper.

References

- [1] Kayisli, K., 2023. Super twisting sliding mode-type 2 fuzzy MPPT control of solar PV system with parameter optimization under variable irradiance conditions. *Ain Shams Engineering Journal*, 14(1), p.101950.
- [2] Sheeba, M.S., Sivakumar, J., Kirubakaran, D., Roseline, J.F., Ezhilarasan, D. and Gomathi, S., 2023, August. Mppt based Model Predictive Controlled Interleaved Boost Converter. In *2023 5th International Conference on Inventive Research in Computing Applications (ICIRCA)* (pp. 1826-1831). IEEE.
- [3] Nechakhin, V., Kalinina, I. and Gozhyj, A., 2023, October. Hyperparameter Optimization of LSTM MPPT Controller for Solar Power Plants. In *2023 IEEE 18th International Conference on Computer Science and Information Technologies (CSIT)* (pp. 1-4). IEEE.
- [4] Tyagi, A., Bihari, S.P., Chaurasia, G.S. and Choudhury, U., 2023, November. MPPT Controller Designed for RBFN-Based Hybrid Energy System. In *2023 3rd International Conference on Advancement in Electronics & Communication Engineering (AECE)* (pp. 1032-1038). IEEE.
- [5] Yilmaz, M., Celikel, R. and Gundogdu, A., 2023. Enhanced photovoltaic systems performance: anti-windup PI controller in ANN-based ARV MPPT method. *IEEE Access*.
- [6] Hameed, A.R., Aftan, A.O. and Kudher, N.A., 2023, September. A structured review of MPPT Techniques for Photovoltaic systems. In *AIP Conference Proceedings* (Vol. 2804, No. 1). AIP Publishing.
- [7] Rashid, M.F., Azhar, A., Khan, S.A., Afzal, S. and Ashraf, I., 2023, February. Single-Stage & Single-Phase Grid Integrated Solar PV System Fed with MPPT Controller. In *2023 International Conference on Power, Instrumentation, Energy and Control (PIECON)* (pp. 1-6). IEEE.
- [8] Shanmugam, Y., Narayanamoorthi, R., Vishnuram, P., Savio, D., Yadav, A., Bajaj, M., Nauman, A., Khurshaid, T. and Kamel, S., 2023. Solar-powered five-leg inverter-driven quasi-dynamic charging for a slow-moving vehicle. *Frontiers in Energy Research*, 11, p.1115262.
- [9] Raj, P.J., Prabhu, V.V., Krishnakumar, V. and Anand, M.C.J., 2023. Solar Powered Charging of Fuzzy Logic Controller (FLC) Strategy with Battery Management System (BMS) Method Used for Electric Vehicle (EV). *International Journal of Fuzzy Systems*, 25(7), pp.2876-2888.
- [10] Naser, A.T., Mohammed, K.K., Ab Aziz, N.F., binti Kamil, K. and Mekhilef, S., 2024. Improved coot optimizer algorithm-based MPPT for PV systems under complex partial shading conditions and load variation. *Energy Conversion and Management: X*, 22, p.100565.
- [11] Regaya, C.B., Hamdi, H., Farhani, F., Marai, A., Zaafour, A. and Chaari, A., 2024. Real-time implementation of a novel MPPT control based on the improved PSO algorithm using an adaptive factor selection strategy for photovoltaic systems. *ISA transactions*, 146, pp.496-510.
- [12] Mazumdar, D., Biswas, P.K., Sain, C., Ahmad, F., Ustun, T.S. and Kalam, A., 2024. Performance analysis of drone squadron optimisation based MPPT controller for grid implemented PV battery system under partially shaded conditions. *Renewable Energy Focus*, 49, p.100577.
- [13] Nagadurga, T., Devarapalli, R. and Knypinski, Ł., 2023. Comparison of Meta-Heuristic Optimization Algorithms for Global Maximum Power Point Tracking of Partially Shaded Solar Photovoltaic Systems. *Algorithms*, 16(8), p.376.

- [14] Hichem, L., Leila, M. and Amar, O., 2024. The effectiveness of a hybrid MPPT controller based on an artificial neural network and fuzzy logic in low-light conditions. *Bulletin of Electrical Engineering and Informatics*, 13(3), pp.1453-1464.
- [15] Hussain, M.T., Sarwar, A., Tariq, M., Urooj, S., BaQais, A. and Hossain, M.A., 2023. An evaluation of ANN algorithm performance for MPPT energy harvesting in solar PV systems. *Sustainability*, 15(14), p.11144.
- [16] Bharathi, G., Mahitha, P.S., Sree, K.B., Sri, K.S.S. and Rani, U.U., 2024, July. Fuzzy Based Solar MPPT for Electric Vehicle Application. In *IOP Conference Series: Earth and Environmental Science* (Vol. 1375, No. 1, p. 012005). IOP Publishing.
- [17] Mutia, A., Abdullah, D., Kraugusteeliana, K., Pramono, S.A. and Sama, H., 2023. Simulation of solar panel maximum power point tracking using the fuzzy logic control method. *Majlesi Journal of Electrical Engineering*, 17(2), pp.29-39.
- [18] Bhattacharjee, R., Deb, A. and Adhikary, N., 2023, November. A Comparative Performance Analysis of P&O and ANN Algorithm Based MPPT Energy Harvesting in PV Systems. In *2023 7th International Conference on Computation System and Information Technology for Sustainable Solutions (CSITSS)* (pp. 1-6). IEEE.
- [19] Bimazlim, M.A.S., Charin, C., Ismail, B. and Jusman, Y., 2024. A Study on Maximum Power Point Tracking (MPPT) Converters for Solar Energy Harvesting. *Journal of Advanced Research in Applied Sciences and Engineering Technology*, pp.278-289.
- [20] Refaat, A., Khalifa, A.E., Elsakka, M.M., Elhenawy, Y., Kalas, A. and Elfar, M.H., 2023. A novel metaheuristic MPPT technique based on enhanced autonomous group Particle Swarm Optimization Algorithm to track the GMPP under partial shading conditions-Experimental validation. *Energy Conversion and Management*, 287, p.117124.
- [21] Hussaian Basha, C., Palati, M., Dhanamjayulu, C., Muyeen, S.M. and Venkatareddy, P., 2024. A novel on design and implementation of hybrid MPPT controllers for solar PV systems under various partial shading conditions. *Scientific Reports*, 14(1), p.1609.
- [22] Mariprasath, T., Basha, C.H., Khan, B. and Ali, A., 2024. A novel on high voltage gain boost converter with cuckoo search optimization based MPPTController for solar PV system. *Scientific Reports*, 14(1), p.8545.
- [23] Manna, S., Singh, D.K., Akella, A.K., Kotb, H., AboRas, K.M., Zawbaa, H.M. and Kamel, S., 2023. Design and implementation of a new adaptive MPPT controller for solar PV systems. *Energy Reports*, 9, pp.1818-1829.
- [24] Viswa Teja, A., Razia Sultana, W. and Salkuti, S.R., 2023. Performance explorations of a PMS motor drive using an ANN-based MPPT controller for solar-battery powered electric vehicles. *Designs*, 7(3), p.79.
- [25] Mallat, M., Kechiche, O.B.H.B., Ezzeddine, K. and Hamouda, M., 2023, October. AN Optimized Genetic Algorithm (GA)-Based MPPT for Off-Grid Solar Photovoltaic System. In *2023 IEEE International Conference on Artificial Intelligence & Green Energy (ICAIGE)* (pp. 1-5). IEEE.
- [26] Areola, R.I., Aluko, O.A. and Dare-Adeniran, O.I., 2023. Modelling of Adaptive Neuro-fuzzy Inference System (ANFIS)-Based Maximum Power Point Tracking (MPPT) Controller for a Solar Photovoltaic System. *Journal of Engineering Research and Reports*, 25(9), pp.57-69.
- [27] Sakthivadivel, D., K. Balaji, D. Dsilva Winfred Rufuss, S. Iniyan, and L. Suganthi. "Solar energy technologies: principles and applications." In *Renewable-energy-driven future*, pp. 3-42. Academic Press, 2021.
- [28] Moyo, Ranganai T., Pavel Y. Tabakov, and Sibusiso Moyo. "Design and modeling of the ANFIS-based MPPT controller for a solar photovoltaic system." *Journal of Solar Energy Engineering* 143, no. 4 (2021): 041002.
- [29] Issa, H. A., H. J. Mohammed, L. M. Abdali, and A. G. Al Bairmani. "Mathematical modeling and controller for PV system by using MPPT algorithm." *Dimension (cm)* 158, no. 8.08 (2021): 4.
- [30] Hichem, Louki, Omeiri Amar, and Merabet Leila. "Optimized ANN-fuzzy MPPT controller for a stand-alone PV system under fast-changing atmospheric conditions." *Bulletin of Electrical Engineering and Informatics* 12, no. 4 (2023): 1960-1981.
- [31] Mohamed, A. Eltawil, and Zhao Zhengming. "MPPT techniques for photovoltaic applications." *Renewable and Sustainable Energy Reviews* 25, no. 3 (2013): 793-813.
- [32] Mirjalili S, Gandomi AH, Mirjalili SZ, Saremi S, Faris H, Mirjalili SM (2017) Salp swarm algorithm: A bio-inspired optimizer for engineering design problems. *Adv Eng Softw* 114:163–191.
- [33] Zand, Sanaz Jalali, Saleh Mobayen, Hamza Zad Gul, Hossein Molashahi, Mojtaba Nasiri, and Afef Fekih. "Optimized fuzzy controller based on cuckoo optimization algorithm for maximum power-point tracking of photovoltaic systems." *IEEE Access* 10 (2022): 71699-71716.
- [34] Alizadeh, Ali, Farhad Soleimanian Gharehchopogh, Mohammad Masdari, and Ahmad Jafarian. "An improved hybrid salp swarm optimization and African vulture optimization algorithm for global

optimization problems and its applications in stock market prediction." *Soft Computing* 28, no. 6 (2024): 5225-5261.

- [35] Rustagi, Krish, Pranav Bhatnagar, Rishabh Mathur, and Indu Singh. "Hybrid salp swarm and grey wolf optimizer algorithm-based ensemble approach for breast cancer diagnosis." *Multimedia Tools and Applications* (2024): 1-25.